Viser Technology Pte. Ltd.
Research and Application of Materials Science
DOI: 10.33142/rams.v4i1.8460

Research Article Open Access

Efficient bio-assembled nanogenerator fabricated from chicken bone epidermis

Yanran MA, Yongfa WANG, Li LI, Chunchang WANG*

Laboratory of Dielectric Functional Materials, School of Materials Science & Engineering, Anhui University, Hefei 230601, China.

***Corresponding Author:** Chunchang WANG, E-mail addresses: ccwang@ahu.edu.cn*

Abstract:
Using biological self-powered materials as a new energy source to replace traditional batteries to power micro-electronic devices is a current research hotspot. We herein fabricate a piezoelectric bio-nanogenerator from chicken bones. The nanogenerator can output a voltage of 1.25 V and a current of 9 nA after being subjected to a pressure of 30 N. This research facilitates an in-depth understanding of bio-nanogenerators and provides a new strategy for reusing bio-waste.
Keywords: *nanogenerator; collagen; piezoelectric; chicken bone epidermis*

1 Introduction

As the energy crisis becomes increasingly severe, the exploration of green and renewable energy sources subsequently received wide attention in various fields. In addition to the traditional energy sources such as coal, natural gas, oil, nuclear energy, as well as green energy sources such as wind, hydro, and solar power that are currently being widely used in the world. On a smaller scale, many scientists are focusing on energy harvesting utilized in our daily life. Researchers have now made some progress in collecting and converting piezoelectric and frictional electricity [1]. The self-powered nanogenerators based on piezoelectric materials have been developed and widely used in fields such as piezoelectric ceramics [1-4] and synthetic polymers [5-7]. However, inorganic power generation materials have some defects in the preparation process, such as high energy consumption, complicated production process, and serious environmental contamination. Therefore, many researchers have turned their attention to biological piezoelectric materials. Piezoelectricity is found in many organs made of biological materials that make up the animal body, such as bone, skin, cellulose, virus, protein, nucleotide and so on [8].

Biological materials are often easily obtained in large quantities and are renewable and less polluting to the environment. Biological piezoelectric materials have not only the high flexibility and toughness of organic materials but also biological compatibility, which is another research hotspot now.

As one of the most abundant renewable resources, biomaterials have an extremely wide range of application scenarios. Compared with conventional polymers, natural biomaterials have unparalleled advantages, namely abundant resources, low prices, simple preparation processes, high energy conversion efficiency, environmental friendliness, and excellent degradability. Problem arises with bio-waste, which can be easily obtained in food production and processing, industrial materials, medical materials, etc. Thus, a large amount of bio-waste is produced every day in these production processes, and how to deal with this bio-waste in the maximum utilization is one of the challenges in this field. Based on the main constituents of bio-waste such as proteins [9], cellulose [10], gelatin [11], chitosan [12], and so on, previous reports have discovered that they can be reused in bio-piezoelectricity. Therefore, we can use bio-waste, for instance, fish scale[13], fish swim bladder[14], and prawn shell [12], to fabricate nanogenerators by simple design and treatment and reduce pollution from traditional energy and electronic waste products. Besides, the nanogenerators based on micro and nanostructures of biomaterials have extremely high sensitivity and electrical output characteristics and can be designed as implantable medical devices or power sources for a wide range of uses considering the degradable properties and excellent biocompatibility of biomaterials [15].

As one of the world's major sources of edible meat, chickens produce a large amount of bone waste every year, and its epidermis is mainly composed of type Ⅰ

Received on April 3, 2022; Accepted on April 23, 2022

collagen which has piezoelectric properties. To our knowledge, piezoelectric nanogenerators fabricated by bone materials are not reported yet. Therefore, chicken bone was chosen as the raw material to prepare bio-nanogenerators. In this study, we fabricated a piezoelectric nanogenerator using chicken bone epidermis (CBENG). The output performance of the CBENG was compared with reported bio-nanogenerators, and the results were listed in Table 1. The raw materials of those reported bio-nanogenerators maintained their natural structures after chemical treatment. The categories, structures, and effective piezoelectric component have an effect on the piezoelectricity of these bio-piezoelectric materials. The CBENG generated an output voltage of 1.25 V and an output current of 9 nA at a pressure of 30N with an impact frequency of 1 Hz. It took 900 seconds to charge the 4.7 μF capacitor to 1.37 V. The CBENG can generate an output power density of 0.01 μW/cm^2 and supply power to small devices like timer through rectifier bridge. The output voltage and current were increased with the rising pressure and impact frequency which proves great sensitivity of CBENG to external pressure changes.

Table 1 Comparison of output performances between the CBENG and other reported piezoelectric nanogenerators based on biomaterials

Material	Effective area	Pressure	Voltage	Current
Native cellulose microfiber[10]	Not supplied	40 kPa	30 V	500 nA
Prawn shell[12]	1.5 ×1 cm^2	12 kPa	4.4V	3.7 nA
Fish scale[13]	1.5 ×1 cm^2	0.17 MPa	4 V	1.5 μA
Fish swim bladder[14]	7 ×3 cm^2	1.4 MPa	10 V	51 nA
Ginkgo tree leaves[16]	Not supplied	16 N	131 V/cm^3	2.5 μA/cm^3
Chicken feather fiber[17]	Not supplied	0.31 MPa	10 V	1.8 mA /cm^2
This work	2.5 ×1.5 cm^2	30N	1.25 V	9 nA

2 Experiment

2.1 Chicken bone treatment

The chicken bone was collected from the fresh food market. The bone treatment and the process of nanogenerator fabrication are shown in Figure 1(a). The chicken bone was cleaned thoroughly with deionized water and dried at 50℃ for 10 hours. For the purpose of demineralization, the bone was soaked in 5 wt% citric acid solution and 0.5 M EDTA for 12 hours in turn [13,18-19]. Then the softened layer was peeled from the surface of the chicken bone and subsequently dried at 50℃ for 10 hours. CBE was sheared into a rectangle for electrode fabrication, which can be seen in Figure 1(b).

2.2 Nanogenerator fabrication

To make a stable nanogenerator, gold (Au) electrodes (with an effective area of ～375 mm^2) were sputtered on both sides of the CBE film. Cu foil was stuck to Au electrodes. Thin copper wires were attached to the Cu foil. Finally, the nanogenerator was sealed to avoid the effect of moisture in the air by a polydimethylsiloxane (PDMS) (DOWSIL, 184 Silicone Elastomer) layer. The PDMS layer is made by mixing the solidified agent in a 1:10 ratio, degassing and curing at room temperature for 15 hours. Figure 1 (c) shows the picture of the CBE made nanogenerator.

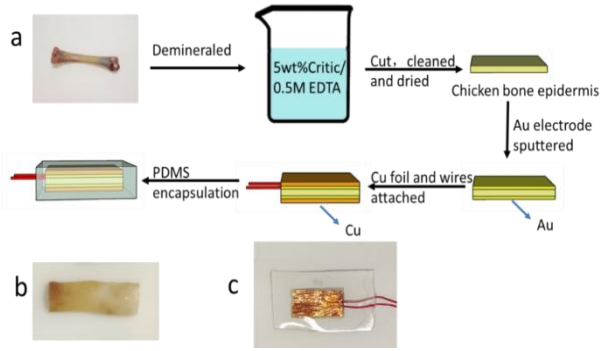

Figure 1 (a) The process of the demineralization and nanogenerator fabrication of chicken bone; (b) A rectangular demineralized chicken bone epidermis; (c) A nanogenerator based on the chicken bone epidermis

2.3 Material characterizations

The structure of the CBE was investigated by X-ray diffraction (XRD, Rigaku Smartlab Beijing Co, Beijing, China) with Cu K α radiation. The detailed cross-section morphologies of the CBE were analyzed by a field emission scanning electron microscope (FESEM, Regulus 8230, Hitachi Co, Japan). The functional groups were analyzed by Fourier microscopy (Vertex80+ Hyperon2000, Bruker, Germany). The dielectric properties of the CBE were gauged by a Wayne Kerr 6500B impedance analyzer (Wayne Kerr Electronic Instrument Co., Shenzhen, China) with Partulab DMS-2000 dielectric measurement system (Partulab Technology Co, Wuhan, China). The sample for dielectric properties characterization was sprayed circular Au electrodes with 6 mm diameter to both sides. The ferroelectric properties of the CBE were tested by a ferroelectric hysteresis measurement tester (MultiFerroic II, Radiant Technologies Inc., Albuquerque, New Mexico) at room temperature and a frequency of 10 Hz. The open circuit voltage and short-circuit current of the CBENG were tested by an electrometer (Model 6514 Programmable Electrometer, Keithley, America). In order to avoid the interference to the test result caused by friction between the PDMS and exterior, the CBENG was wrapped with insulating tape and copper foil with wire grounding.

3 Results and discussion

3.1 Characterization

It has been confirmed in many previous researches that the main components of bone are hydroxyapatite and collagen [18, 20]. Inorganic component with hydroxyapatite as the main component was separated by immersed in citric acid and EDTA solutions [18-19, 21]. To confirm the collagen type of the CBE and analyze its structure, it was investigated by XRD and Fourier Transform infrared spectroscopy (FTIR). As illustrated in Figure 2(a), two main crystallization peaks were located at 2θ = 7.43 °and 21.51 °in the XRD pattern of the demineralized CBE. The feature peak at 7.43 ° represents a highly crystalized structure in collagen. The broad peak at 21.51 ° is due to the amorphous composition of collagen [14]. Meanwhile, there were shoulder peaks at 2θ = 30.81° and 38.95° which are caused by amino acid residue of triple-helical structure[14]. These characteristic peaks prove the crystallization behavior of the CBE. The crystallinity is about 27.25% calculated by the Fourier deconvolution calculation. The stable crystalline structure is derived from peptide chains in collagen that relies on many intramolecular and intermolecular hydrogen bonds to form ordered and dense structures.

The cross-section SEM images of the CBE with different multiples are shown in Figure 2 (b, c). Notably, the CBE exhibits a relatively loose layered fiber structure as shown in Figure 2(b). In Figure 2(c), a further enlarged view reveals that the structural composition of the CBE is composed of superimposed collagen fibrils.

The chemical composition of the CBE was tested by FTIR spectrum. The FTIR spectra of the CBE with the attribution of characteristic peaks are shown in Figure 2(d). The figure shows amide I, II, and III bands at 1633, 1548, and 1260 cm^{-1}, respectively. The assignments of amide I band are stretching vibration (ν) of carbon-oxygen double bond (ν(C=O)) or hydrogen bonding. Amide II band is caused by stretching vibrations of carbon-nitrogen bond (ν(C-N)) coupled with bending vibrations (δ) of nitrogen-hydrogen bond (δ(N-H)) [22].The absorption band at 1452 cm^{-1} and amide III band at 1260 cm^{-1} are attributed to δ(CH_2) and δ(N-H), respectively [16]. The existence of triple-helical structure in the CBE collagen is supported by the ratio of absorption band at 1260 cm^{-1} (amide III) and 1452 cm^{-1} (δ (CH_2)), which is 1.034, approximately equal to 1[23-24].Amide A band is usually at 3400-3440 cm^{-1}, and it is generally associated with N-H stretching vibrations (ν (N-H)) and hydrogen bonding on the polypeptide within the CBE collagen. The position of the characteristic peak towards low wavenumber 3287 cm^{-1} is due to the involvement of stretching vibrations of double-bonded carbonic acid (ν(C=N)) and N-H on the peptide in the formation of hydrogen bonds[24]. The observation of two vibration bands at 2980 and 2860 cm^{-1} are related to the asymmetric and symmetric vibrational modes of CH_2 (ν(CH_2)), respectively. The two combined bands prove that amide B band is existed in collagen fibers. The above analysis demonstrates the existence of the triple-helical structure in collagen of the CBE and the structural stability of collagen fibrils in the CBE because of its regular bonding and crystallinity. Collagen fibers are combined by hydrogen bonding to form type I collagen fiber bundles, which finally constitute a laminar structure. This structural feature facilitates the formation of

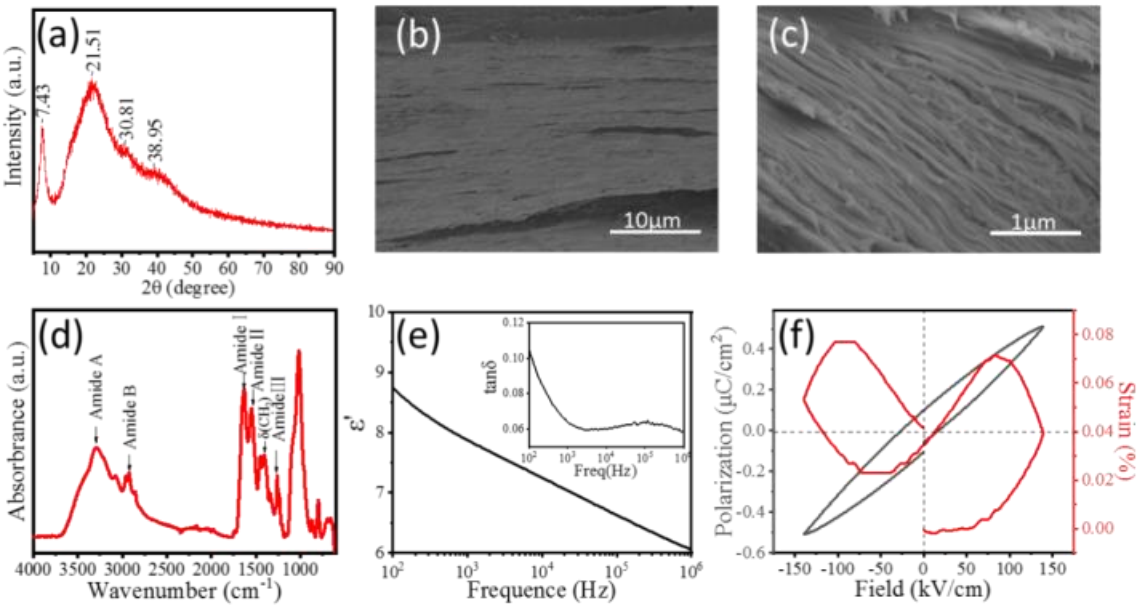

Figure 2 (a) XRD spectra of the CBE. (b, c) SEM of cross-section images. (d) FTIR patterns of the CBE. (e) Frequency dependent tan δ and ε' in the frequency range from 10^2 to 10^6 Hz. (f) The standard P-E loop and S-E loop of the CBE

spontaneous polarization, which results in the piezoelectric effect [25-26]. Quarterly interlacing of collagen molecules gives the typical axial and cyclical organization of collagen protofibrils, and protofibrils are further assembled to form collagen fibers. The formation of hydrogen bonds between multi-peptide chains is crucial for piezoelectricity. Collagen is a natural electret or bio-electret material because of the inherent uniaxial polar orientation of molecular dipoles leading to polarization and piezoelectricity [27]. In summary, the results prove the existence of the helical structure and the tripeptide sequence of Gly-Pro-Y in the collagen of the CBE as shown in Figure 3 [27].

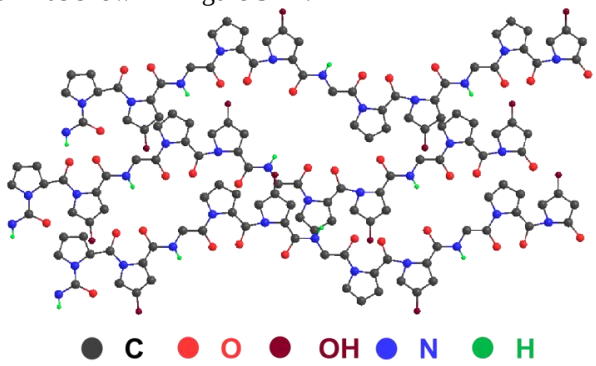

Figure 3 The schematic illustration of peptide chains of collagen in CBE

In order to illustrate this point, we measured the dielectric dissipation factor (tan δ) and dielectric constant (ε') of the CBE in the frequency range from 10^2 to 10^6 Hz, and the results are shown in Figure 2(e). The dielectric constant is 8.5 at 100 Hz and monotonically decreases with increasing frequency. The tan δ curve registers a pear at 2×10^5 Hz and increases rapidly with decreasing frequency. The tan δ pear suggests that there exists a relaxation in the CBE. The low-frequency increase in tan δ indicates a Maxwell-Wagner relaxation caused by the space charge. The results evidence that the CBE is able to store and release electric charge. To further confirm the ferroelectricity and piezoelectricity of the CBE, hysteresis of polarization (P) with electric field (E) was measured as shown in Figure 2(f). It demonstrates a remnant polarization (Pr) of 0.1 μC/cm^2. The corresponding strain (S) - electric field (E) hysteresis loop shows a butterfly shape as shown in Figure 2(f). The above proved the existence of inverse piezoelectric effect in the CBE.

3.2 Working principle

It has been confirmed that the reason of piezoelectricity in bone is the existence of tropocollagen, which is the basic structural composition unit of collagen [28]. This is due to the particular arrangement of the polypeptide chain in tropocollagen [29]. The tropocollagen consists of three polypeptide chains in a triple-helical structure. When subjected to external mechanical pressure, the triple-helical structure will uncoil. As a result, the hydroxyproline side chains will become more inclined to the long axis of the tropocollagen which reorients the polar groups of the molecule. At the same time, the dipole moment changed under external pressure. The above leads to the polarization of the CBE and piezoelectric effect. The piezoelectric mechanism is shown in Figure 4. The generation of electricity in the CBENG results from piezoelectric mechanism, of which the CBE generates an electric field and induces opposite charges in the upper and lower electrodes because of the mechanical deformation and polarization of the CBE. Due to the fact that CBE is a dielectric material, electrons can only pass through the external load. When it is pressed by external pressure, it will generate a positive output current. When deformation reaches the maximum, the output current decreases to 0 nA. As the nanogenerator is releasing, the free charge reverses to form the opposite current to balance the cumulative charge at both ends of the external circuit.

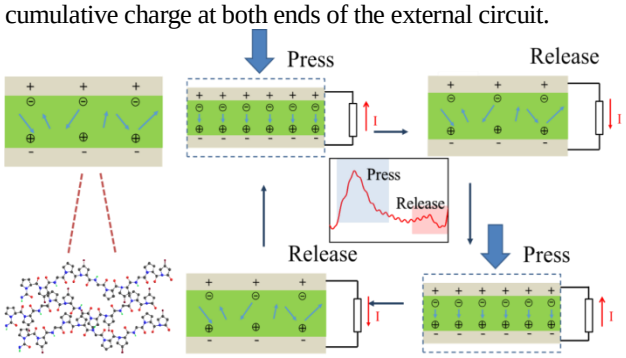

Figure 4 Schematic diagram of the CBE piezoelectricity

3.3 CBENG output

To test the output performance of the nanogenerator, we used an electrometer to measure its output voltage and output current under the steady pressure of the electric motor. The results are demonstrated in Figure 5.

The output performance of the nanogenerator was tested by periodical electric motor impact vertically on the electrodes under a mechanical pressure of 30 N. As shown in Figure 5(a, b), the output voltage of the CBENG is 1.25 V and the output current is 9 nA. In the reverse connection, the output amplitude of the CBENG is same but the curve is in opposite direction compared with the forward connection. It is due to piezoelectric effect. In order to measure the output current and calculate the power density of the CBENG under different resistive loads, a variable value resistor box was connected to the nanogenerator to form a closed circuit. In Figure 5(c), the current decreases with the increase of the resistance. When resistance reached 5×10^7 Ω, the output power shows a maximum value of 0.01 μW/cm^2 as deduced according to the following formula:

$$P = U^2 / RA \quad (1)$$

where A is the effective area of the CBENG (25mm×15mm), U is the output voltage in the closed circuit, R is the external load resistance. In the output test, CBENG exhibited better output performance when subjected to vertical mechanical stress on the electrode

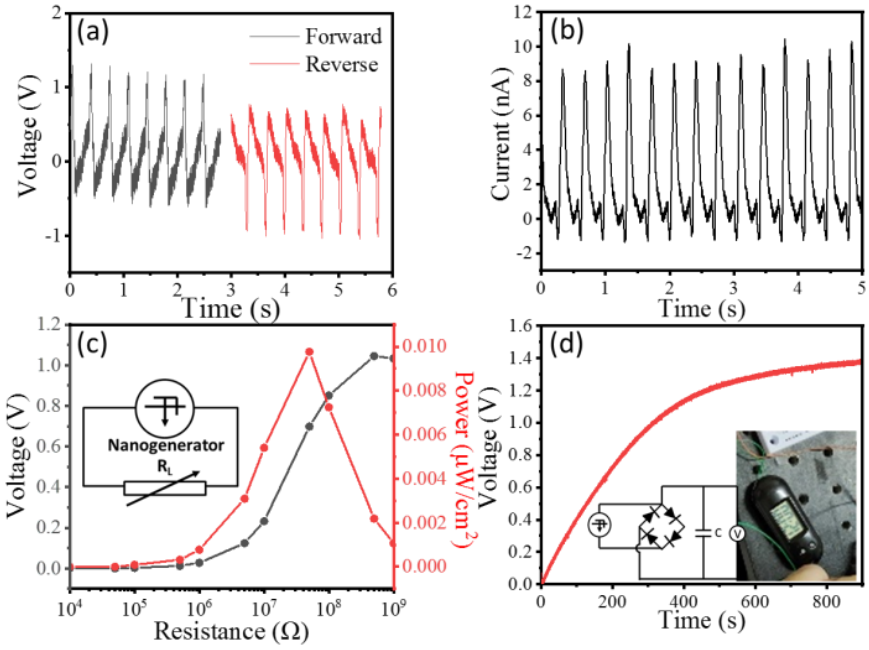

Figure 5 Output performance of the CBENG. (a) Output voltage and (b) output current under a constant pressure of 30 N. (c) Output voltage and output power density on the different external load resistance (R_L). (d) A capacitor charging and driving an electronic timer performance

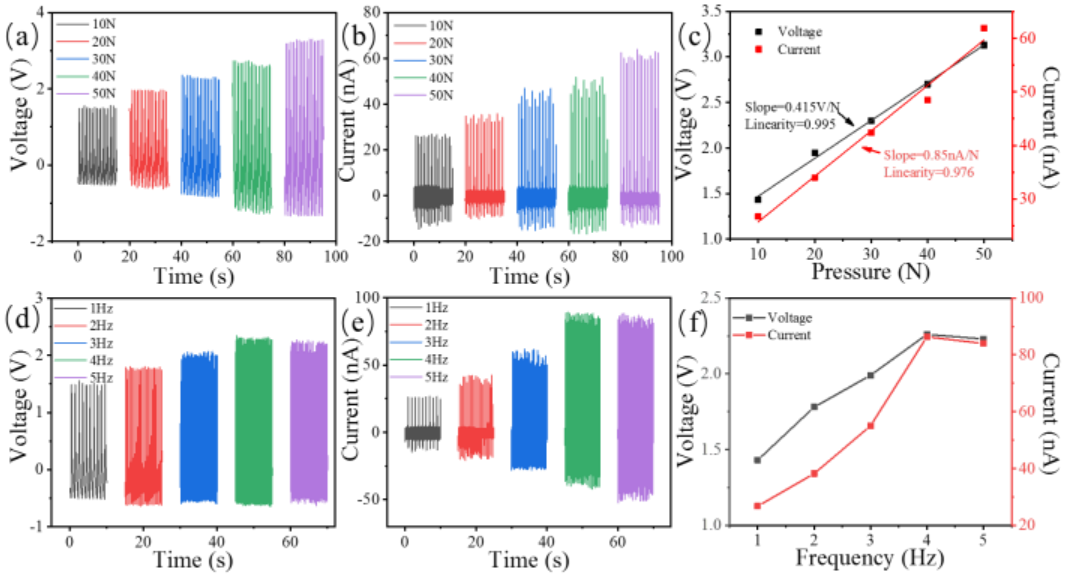

Figure 6 (a) Output voltage and (b) output current of CBENG under diverse external pressure. (c) Dependence of output voltage and current of the CBENG on the external pressure. (d) Output voltage and (e) output current of CBENG under different impact frequency. (f) Dependence of output voltage and current of the CBENG on the impact frequency

surface. It is expected that the molecular structure is changed under an applied stress, which, in turn, gives rise to the piezoelectricity of collagen.

To test the charging performance of the CBENG, a rectifier bridge and a 4.7 μF capacitor in closed circuit were connected to the generator. The schematic circuit diagram used to charge the 4.7 μF capacitor is shown in Figure 5(d). It took 900 seconds to charge the 4.7 μF capacitor to 1.37 V. It can supply power to small devices like timer through rectifier bridge as shown in Figure 5(d).

In order to systematically study the output properties of the CBENG (A=3×2 cm^2), it was tested under diverse external pressure and different impact frequency. As Figs. 6(a-c) show, with the increase of external pressure, the output voltage and current were linear increased. Through linear fit calculation, the slope of output voltage is 0.415

V/N and the linearity is 0.995. The slope of output current is 0.85 nA/N and the linearity is 0.976. It performed the great pressure sensing property of CBENG in a broad range of pressure. The CBE is polarized under the external force and leads to the appearance of bound charges with opposite polarities on the surfaces of both ends of the CBE. The charge density is proportional to the external mechanical force. Therefore, the output voltage and current are positively correlated with the external force which proved piezoelectric effect in CBE. As Figs. 6(d-f) show, with the increase of impact frequency, the output voltage and current increased gradually to a steady level. Due to the high impact frequency, the CBE can't recover its shape in time to cause the voltage to stop increasing. CBENG exhibits good pressure sensing sensitivity and can be used as an excellent pressure sensor. It also can be used to collect and transform mechanical energy to charge small devices.

4 Conclusion

In conclusion, we proved that CBE can be used as biological piezoelectric material and fabricated a flexible and biocompatible nanogenerator based on it. The main component, microstructure, dielectric properties of chicken bone epidermis, and the output performance of the nanogenerator were investigated. The nanogenerator can output a voltage of 1.25 V and a current of 9 nA after being subjected to a pressure of 30 N. It can be used to charge low-power devices by a rectifier bridge and measure pressure as pressure sensor because of its sensitivity of external force. Authors believe it will provide further insights into the processing of bio-wastes.

Declaration

The authors report no declarations of interest.

Acknowledgements

This work was financially supported by the National Natural Science Foundation of China (Grant Nos. 51872001 and 12174001).

References

[1] Su Y Li, W Yuan, L Chen, C Pan, H, Xie, G Conta, G, Ferrier, S Zhao, X Chen, G Tai, H Jiang, Y Chen. J Piezoelectric fiber composites with polydopamine interfacial layer for self-powered wearable biomonitoring. Nano Energy 2021(89): 106321.

[2] Su, H Wang, X Li, C Wang, Z Wu, Y Zhang, J Zhang, Y Zhao, C Wu, J Zheng. H Enhanced energy harvesting ability of polydimethylsiloxane-BaTiO3-based flexible piezoelectric nanogenerator for tactile imitation application. Nano Energy 2021(83): 105809.

[3] Wang, Z Yuan, X Yang, J Huan, Y Gao, X Li, Z Wang, H Dong. S 3D-printed flexible, Ag-coated PNN-PZT ceramic-polymer grid-composite for electromechanical energy conversion. Nano Energy 2020(73): 104737.

[4] Ji, S. H Lee, W Yun, J. S All-in-One Piezo-Triboelectric Energy Harvester Module Based on Piezoceramic Nanofibers for Wearable Devices. ACS applied materials & interfaces 2020, 12 (16): 18609-18616.

[5] Rahman, M. A Rubaiya, F Islam, N Lozano, K Ashraf, A Graphene-Coated PVDF/PAni Fiber Mats and Their Applications in Sensing and Nanogeneration. ACS applied materials & interfaces 2022, 14 (33): 38162-38171.

[6] Su, Y Chen, C Pan, H Yang, Y Chen, G Zhao, X Li, W Gong, Q Xie, G Zhou, Y Zhang, S Tai, H Jiang, Y Chen, J Muscle Fibers Inspired High-Performance Piezoelectric Textiles for Wearable Physiological Monitoring. Advanced Functional Materials 2021, 31 (19): 2010962.

[7] Zhao, J Li, F Wang, Z Dong, P Xia, G Wang, K Flexible PVDF nanogenerator-driven motion sensors for human body motion energy tracking and monitoring. Journal of Materials Science: Materials in Electronics 2021, 32 (11): 14715-14727.

[8] Cao, L Qiu, X Jiao, Q Zhao, P Li, J Wei, Y. Polysaccharides and proteins-based nanogenerator for energy harvesting and sensing: A review. International journal of biological macromolecules 2021, 173, 225-243.

[9] Chang, T.-H Peng, Y.-W Chen, C.-H Chang, T.-W Wu, J.-M Hwang, J.-C Gan, J.-Y Lin, Z.-H. Protein-based contact electrification and its uses for mechanical energy harvesting and humidity detecting. Nano Energy 2016(21): 238-246.

[10] Alam, M. M Mandal, D. Native Cellulose Microfiber-Based Hybrid Piezoelectric Generator for Mechanical Energy Harvesting Utility. ACS applied materials & interfaces 2016, 8 (3): 8-1555.

[11] Ghosh, S. K Adhikary, P Jana, S Biswas, A. Sencadas, V. Gupta, S. D Tudu, B Mandal, D. Electrospun gelatin nanofiber based self-powered bio-e-skin for health care monitoring. Nano Energy 2017(36): 166-175.

[12] Ghosh, S. K.; Mandal, D. Bio-assembled, piezoelectric prawn shell made self-powered wearable sensor for non-invasive physiological signal monitoring. Applied Physics Letters 2017, 110 (12): 123701.

[13] Ghosh, S. K Mandal, D. High-performance bio-piezoelectric nanogenerator made with fish scale. Applied Physics Letters 2016, 109 (10): 103701.

[14] Ghosh, S. K Mandal, D. Efficient natural piezoelectric nanogenerator: Electricity generation from fish swim bladder. Nano Energy 2016(28): 356-365.

[15] Chen, S Wu, N Lin, S Duan, J Xu, Z Pan, Y Zhang, H Xu, Z Huang, L Hu, B Zhou, J. Hierarchical elastomer tuned self-powered pressure sensor for wearable multifunctional cardiovascular electronics. Nano Energy 2020(70): 104460.

[16] Shao, D Wang, C Li, W Lu, L Lu, J Yang, W. Natural ginkgo tree leaves as piezo-energy harvesters. Journal of Materials Chemistry C 2022, 10 (40): 15016-15027.

[17] Kar, E Barman, M Das, S Das, A Datta, P Mukherjee, S Tavakoli, M Mukherjee, N Bose, N. Chicken feather fiber-based bio-piezoelectric energy harvester: an efficient green energy source for flexible electronics. Sustainable Energy & Fuels 2021, 5 (6): 1857-1866.

[18] Cao, S Wang, Y Xing, L Zhang, W Zhou, G. Structure and

physical properties of gelatin from bovine bone collagen influenced by acid pretreatment and pepsin. Food and Bioproducts Processing 2020(121): 213-223.

[19] Wilson, T Szpak, P. Acidification does not alter the stable isotope composition of bone collagen. PeerJ 2022(10):e13593.

[20] Liu, H.; Huang, K., Structural Characteristics of Extracted Collagen from Tilapia (Oreochromis mossambicus) Bone: Effects of Ethylenediaminetetraacetic Acid Solution and Hydrochloric Acid Treatment. International Journal of Food Properties 2014, 19 (1): 63-75.

[21] Jaziri, A. A Shapawi, R Mohd Mokhtar, R. A Md Noordin, W. N Huda, N. Biochemical analysis of collagens from the bone of lizardfish (Saurida tumbil Bloch, 1795) extracted with different acids. PeerJ 2022(10): e13103.

[22] Muyonga, J. H Cole, C. G. B Duodu, K. G. Characterisation of acid soluble collagen from skins of young and adult Nile perch (Lates niloticus). Food Chemistry 2004, 85 (1): 81-89.

[23] Kaewdang, O Benjakul, S Kaewmanee, T Kishimura, H. Characteristics of collagens from the swim bladders of yellowfin tuna (Thunnus albacares). Food Chem 2014(155): 264-70.

[24] Wang, L. S Shi, Z Shi, B. M Shan, A. S. Effects of dietary stevioside/rebaudioside A on the growth performance and diarrhea incidence of weaned piglets. Animal Feed Science and Technology 2014(187): 104-109.

[25] Guerin, S.; Syed, T. A. M.; Thompson, D., Deconstructing collagen piezoelectricity using alanine-hydroxyproline-glycine building blocks. Nanoscale 2018, 10 (20): 9653-9663.

[26] Ravi, H. K Simona, F Hulliger, J Cascella, M. Molecular Origin of Piezo- and Pyroelectric Properties in Collagen Investigated by Molecular Dynamics Simulations. The Journal of Physical Chemistry B 2012, 116 (6): 1901-1907.

[27] Wu, B Mu, C Zhang, G Lin, W. Effects of Cr3+ on the structure of collagen fiber. Langmuir 2009, 25 (19): 11905-10.

[28] Weiner, S. W. H. D. The Material Bone: Structure-Mechanical Function Relations. Annual Review of Materials Science 1998, 28 (1): 271-298.

[29] Zhou, Z Qian, D Minary-Jolandan, M. Molecular Mechanism of Polarization and Piezoelectric Effect in Super-Twisted Collagen. ACS Biomater Sci Eng 2016, 2(6): 929-936.